Sub-carrier Spacing Detection Algorithm in 5G New Radio Systems

Tong Li(✉), Hang Long, and Li Huang

Wireless Signal Processing and Network Lab, Key Laboratory of Universal Wireless Communication, Ministry of Education, Beijing University of Posts and Telecommunications, Beijing, China
tttli@bupt.edu.cn

Abstract. In 5G New Radio (NR) systems, the configuration of frame is flexible. There are several sub-carrier spacing (SCS) configurable which is different from Long Term Evolution (LTE) systems. During the initial access process, the user equipment cannot know the specific SCS directly before obtaining time and frequency synchronization with the service cell like in LTE systems. Therefore, it is necessary to investigate SCS detection. Based on the cyclostationary of Orthogonal Frequency Division Multiplexing (OFDM) signals, we propose a SCS detection algorithm with correlation operations on OFDM signals. The proposed algorithm is theoretically analyzed and the theoretical expression for the detection error rate is given by integrating theoretical models of the correlation errors. The algorithm is evaluated and analyzed through simulation in different scenarios. The analytical and simulation results show that the proposed algorithm is effective and the performance is roughly consistent with the theoretical analysis results.

Keywords: NR · SCS · Detection

1 Introduction

The 3rd Generation Partnership Project (3GPP) requires 5G New Radio (NR) networks to provide user equipments (UE) access experience with ultra-high network capacity, ultra-high reliability and ultra-low network latency anytime and anywhere [1]. Cell initial access is a process in which the UE can obtain time and frequency synchronization with the servicing cell and detect the physical layer cell ID of the servicing cell. In 5G NR systems, the concept of Synchronization Signal Blocks (SSBs) is newly introduced [2]. In addition, in order to adapt to different business scenarios, the design of frame structure is very flexible and the sub-carrier spacing (SCS) of Orthogonal Frequency Division Multiplexing

Supported by the National Natural Science Foundation of China (NSFC) Project 61931005.

H. Gao et al. (Eds.): ChinaCom 2021, LNICST 433, pp. 322–334, 2022.
https://doi.org/10.1007/978-3-030-99200-2_25

(OFDM) symbols in different frequency bands is flexible and variable [3]. Therefore, the cell search process in 5G NR systems is somewhat different from that in Long Term Evolution (LTE) systems. UE cannot directly learn the SCS of the SSB. To takle this problem, it is necessary to carry out the research of SCS detection. After that, frequency domain synchronization can be obtained.

At present, few studies about SCS detection have been presented thus far in the literature. There are some literatures related to the estimation of OFDM parameters. Based on cyclostationary characteristics, a blind algorithm for estimating carrier frequency and symbol offset of OFDM system in Rayleigh multipath channels is proposed in [4]. In [5], the time symbol duration is determined by exploiting the cyclostationnarity of the symbol. In [6], a blind estimation method of OFDM system parameters is proposed. The method sequentially estimate the sampling frequency, the number of sub-carriers and the cyclic prefix (CP) length in OFDM systems. However, these literatures do not give a specific analysis of detection performance.

Against the above backdrop on SCS detection, we propose a new SCS detection algorithm based on the cyclostationarity of OFDM symbols. When the time delay is the number of effective symbol points corresponding to the actual SCS, the peak value of the correlation calculation can be obtained. Based on this feature, the SCS can be determined. The detection performance of the proposed algorithm is both theoretically analyzed and simulated under multiple scenarios. The simulation results show that the proposed detection algorithm is effective. Furethermore, the simulation results are consistent with their theoretical analysis results.

The remainder of this paper is organized as follows. Section 2 mainly describes the cyclostationarity of OFDM symbols. Section 3 designs and elaborates the proposed algorithm. And the performance is analyzed through theoretical derivation. In Sect. 4, the simulation results of the proposed algorithm are analized and compared with theoretical derivation. Finally, concluding remarks are drawn in Sect. 5.

2 System Model and the Cyclostationarity of OFDM Signals

The received OFDM signals after passing through the Additive White Gaussian Noise (AWGN) channel can be expressed as

$$r(t) = s(t) + n(t), \tag{1}$$

where $s(t)$ is the baseband OFDM signal, $n(t)$ is the zero-mean Gaussian white noise, $n(t) \sim CN(0, \sigma_n^2)$ and σ_n^2 represents the noise power. $s(t)$ is defined as follow

$$s(t) = \sum_{k} \sum_{l=0}^{G-1} c_{k,l} g(t - lT_c - kT_s), \tag{2}$$

where G represents the number of total sampling points of an OFDM symbol, $G = N + D$, N is the number of effective sampling points of an OFDM symbol, D is the length of the CP, T_c and T_s denote the sampling period and the OFDM symbol length, $T_s = GT_c$, $g(t)$ is the rectangular shaped pulse and $c_{k,l}$ represents the l-th sampling point of the k-th symbol in the time-domain. $c_{k,l}$ is defined as follow

$$c_{k,l} = \frac{1}{\sqrt{N}} \sum_{n=0}^{N-1} a_{k,n} \mathrm{e}^{(\mathrm{j}2\pi(\mathrm{l}-\mathrm{D})\mathrm{n}/\mathrm{N})}, l = 0, 1, \cdots, G-1, \tag{3}$$

where $a_{k,n}$ denotes the modulated data on the n-th sub-carrier of the k-th symbol in the frequency-domain. The mean and variance of $a_{k,n}$ are 0 and σ_a^2, respectively. $a_{k,n}$ is mutually independent and identically distributed. Moreover, $a_{k,n}$ has some distribution characteristics as follows

$$E[a_{k,n}] = 0, \tag{4}$$

$$E[a_{k,n} a_{m,l}] = 0, \tag{5}$$

$$E[a_{k,n} a_{m,l}^*] = \sigma_a^2 \delta(k-m) \delta(n-l), \tag{6}$$

where δ is the Dirac function.

OFDM signals have the characteristic of second-order cyclostationarity [7, 8,10]. Use $R_r(t, \tau)$ to denote the autocorrelation function of OFDM signals in time-domain. $R_r(t, \tau)$ can be expressed as follow

$$R_r(t,\tau) = \begin{cases} \sigma_a^2 \sum\limits_k \sum\limits_{l=0}^{G-1} g(t - lT_c - kT_s) \cdot g^*(t - lT_c - kT_s - \tau) + R_n(\tau), & |\tau| < T_c \\ \sigma_a^2 \sum\limits_k \sum\limits_{l=N}^{G-1} g(t - lT_c - kT_s) \cdot g^*(t - lT_c - kT_s - \tau_N) + R_n(\tau), & |\tau_N| < T_c \\ 0, \quad \tau = others \end{cases}, \tag{7}$$

where $\tau_N = |\tau| - NT_c$. As can be seen from (7), the OFDM signal is second-order cyclostationary and the period of autocorrelation function is T_s. The autocorrelation function is formulated by

$$R_r(t,\tau) = \begin{cases} R_r(t + T_c, \tau), & |\tau| < T_c \\ R_r(t + T_s, \tau), & |\tau_N| < T_c \end{cases}. \tag{8}$$

Hence, the autocorrelation function of the OFDM received signal can be expressed in the form of Fourier series. The absolute value of the autocorrelation function is as follow,

$$|R_s^\alpha(\tau)| = \begin{cases} \frac{\sigma_a^2}{T_c} \left| \frac{\sin[\pi\alpha(T_c - |\tau|)]}{\pi\alpha} \right|, & \alpha = m/T_c, |\tau| \le T_c, m \in \mathrm{Z} \\ \frac{\sigma_a^2}{T_s} \left| \frac{\sin(\pi\alpha T_c D)}{\sin(\pi\alpha T_c)} \right| \cdot \left| \frac{\sin[\pi\alpha(T_c - |\tau_N|)]}{\pi\alpha} \right|, & \alpha = m/T_s, |\tau_N| \le T_c, m \in \mathrm{Z} \end{cases}, \tag{9}$$

where α represents a cycle frequency, $\alpha = m/T_s$, $m \in Z$. Therefore, the autocorrelation spectrum of the OFDM signal appears only when $\alpha = m/T_c$ or $\alpha = m/T_s$. If $\alpha = 0$, $R_s(\tau)$ has peaks only under the condition of $\tau = 0$ and $\tau = NT_c$, and the peaks are σ_a^2 and $\sigma_a^2 D/G$, respectively. The autocorrelation results with other time delays are all zero.

3 Description and Analysis of Sub-carrier Spacing Detection Algorithm

3.1 Algorithm Description

In 5G NR systems, SSB does not support the SCS configuration of 60 kHz [9]. In the frequency range 1 (FR1), the SCS that require detection are 15 kHz and 30 kHz. And in the frequency range 2 (FR2), the SCS that require detection are 120 kHz and 240 kHz. Therefore, there are two candidate SCS in each frequency range. Assuming that the number of effective sampling points of an OFDM symbol corresponding to the actual SCS is N_1, and the other is N_2. Use $r(m)$ to represent the sampling results of time-domain received sequence. The autocorrelation result $R_r(l)$ of $r(m)$ can be expressed as

$$R_r(l) = \frac{1}{M}\mathrm{Re}\left[\sum_{m=0}^{M-1} r(m) \cdot r^*(m-l)\right] = \frac{1}{M}\mathrm{Re}\left[\sum_{m=0}^{M-1} R(m,l)\right], \tag{10}$$

where M and l represent the number of the sampling points and time delay of the autocorrelation calculation, respectively. According to theoretical analysis, $R_r(l)$ obtains the peak value only when the time delay l equals N_1. If the time delay l equals N_2, the expectation of the autocorrelation calculation is zero.

The specific flow of the proposed algorithm is as follows.

- Carry out the autocorrelation calculation of the time-domain received sequence based on the time delay N_1 and N_2, respectively. The results are denoted as $R_r(N_1)$ and $R_r(N_2)$.
- Compare the values of $R_r(N_1)$ and $R_r(N_2)$ and decide the SCS corresponding to the larger one.

Apparently, if $R_r(N_2)$ were larger than $R_r(N_1)$, the detection result would definitely be wrong.

3.2 Analysis of Sub-carrier Spacing Detection Algorithm

Considering AWGN channels, there is additive white Gaussian noise $n(t)$ in the system, $n(t) \sim \mathcal{CN}(0, {\sigma_n}^2)$. The autocorrelation function of the received signal consists of three parts. It is expressed as

$$R_r(l) = R_s(l) + R_n(l) + R_{s,n}(l) + R_{n,s}(l), \tag{11}$$

where $R_s(l)$ and $R_n(l)$ represent the autocorrelation function of the useful signal $s(t)$ and the noise $n(t)$, $R_{s,n}(l)$ and $R_{n,s}(l)$ denote the cross-correlation function of useful signal and noise and $R_{s,n}(l) = R^*_{n,s}(l)$. Due to the limited sampling points at the receiving end for correlation calculations, $R_s(N_1)$ or $R_s(N_2)$ cannot get the theoretical peak values $\sigma_a^2 D/G$ and 0. In addition, the autocorrelation result of noise and the cross-correlation result between noise and useful signal cannot reach 0. These are all components of the error.

The autocorrelation function of the useful signal is as follow

$$R_s(l) = \frac{1}{M}\mathrm{Re}\left[\sum_{m=0}^{M-1} s(m)\cdot s^*(m-l)\right] = \frac{1}{M}\mathrm{Re}\left[\sum_{m=0}^{M-1} S(m,l)\right]. \tag{12}$$

We suppose that the time-domain received signal sequence $s(m)$ follows a complex Gaussian distribution, i.e., $s(m) \sim \mathcal{CN}(0, {\sigma_a}^2)$, where ${\sigma_a}^2$ is the variance of the frequency-domain modulation symbols at the transmitter. It is assumed that the different sampling points are independent of each other. Then, the autocorrelation results $R_s(N_1)$ and $R_s(N_2)$ with time delay of N_1 and N_2 are assumed to obey Gaussian distributions. Correlation with delay N_1 involves the autocorrelation of the cyclic prefix (CP), so the mean value of $R_s(N_1)$ is positive. The distribution of $R_s(N_1)$ is expressed as

$$R_s(N_1) \sim \mathcal{N}\left(\frac{\sigma_a^2 D}{G}, \frac{2D{\sigma_a}^4 + N{\sigma_a}^4}{2MG}\right). \tag{13}$$

The mean value $\sigma_a^2 D/G$ is the expected theoretical peak of autocorrelation calculation as described in Sect. 3. While the mean value of the autocorrelation calculation results with N_2 as the time delay is 0. The distribution of $R_s(N_2)$ can be expressed as

$$R_s(N_2) \sim \mathcal{N}\left(0, \frac{{\sigma_n}^4}{2M}\right). \tag{14}$$

The autocorrelation function of noise is formulated by

$$R_n(l) = \frac{1}{M}\mathrm{Re}\left[\sum_{m=0}^{M-1} n(m)\cdot n^*(m-l)\right] = \frac{1}{M}\mathrm{Re}\left[\sum_{m=0}^{M-1} N(m,l)\right]. \tag{15}$$

Since the noise at different sampling points is independent and identically distributed, the mean value and variance of $R_n(l)$ are respectively 0 and $\sigma_n^4/2M$. We suppose that $R_n(l)$ follows a Gaussian distribution, $R_n(l) \sim \mathcal{N}(0, {\sigma_n}^4/2M)$.

The cross-correlation function of useful signal and noise is as follow

$$R_{s,n}(l) = \frac{1}{M}\mathrm{Re}\left[\sum_{m=0}^{M-1} s(m)\cdot n^*(m-l)\right] = \frac{1}{M}\mathrm{Re}\left[\sum_{m=0}^{M-1} SN(m,l)\right]. \tag{16}$$

The useful signal and noise are independent of each other. According to the approximate results of useful signal and noise, the cross-correlation function $R_{s,n}(l)$ is approximated as a Gaussian distribution, $R_{s,n}(\tau) \sim \mathcal{N}\left(0, {\sigma_a}^2{\sigma_n}^2/2M\right)$.

According to the above discription, the detection error rate of SCS under AWGN channel is calculated as

$$\begin{aligned} P_e &= P\left[R_r(N_2) > R_r(N_1)\right] \\ &= P\left\{R_n(N_2) + R_s(N_2) + 2\mathrm{Re}\left[R_{s,n}(N_2)\right]\right. \\ &\quad \left. -R_n(N_1) - R_s(N_1) - 2\mathrm{Re}\left[R_{s,n}(N_1)\right] > 0\right\}. \end{aligned} \tag{17}$$

Let

$$\xi = R_n(N_2) + R_s(N_2) + 2\mathrm{Re}[R_{s,n}(N_2)] - R_n(N_1) - R_s(N_1) - 2\mathrm{Re}[R_{s,n}(N_1)]. \tag{18}$$

According to the above analysis, the distribution of ξ is expressed as

$$\xi \sim \mathrm{N}\left(\frac{-\sigma_a^2 D}{G}, \frac{{\sigma_n}^4 + {\sigma_a}^4 + 2{\sigma_a}^2{\sigma_n}^2}{M} + \frac{D{\sigma_a}^4}{2MG}\right). \tag{19}$$

Therefore, the SCS detection error rate is calculated as

$$\begin{aligned} P_e &= P(\xi > 0) \\ &= Q\left(\frac{\sigma_a^2 D/G}{\sqrt{\frac{{\sigma_n}^4+{\sigma_a}^4+2{\sigma_a}^2{\sigma_n}^2}{M} + \frac{D{\sigma_a}^4}{2MG}}}\right) \\ &= Q\left(\frac{\sigma_a^2 D\sqrt{2M}}{\sqrt{2G^2({\sigma_n}^4+{\sigma_a}^4+2{\sigma_a}^2{\sigma_n}^2)+DG{\sigma_a}^4}}\right). \end{aligned} \tag{20}$$

The detection error rate is related to signal-to-noise ratio (SNR) and the number of sampling points M. Moreover, the detection performance has nothing to do with the specific SCS. When other conditions are the same, the detection performance of different SCS is roughly consistent. In addition, the complexity of the proposed detection algorithm primarily depends on the number of conjugate multiplications M. Therefore, the larger the number of conjugate multiplications, the better the detection performance. However, the complexity also increases at the same time.

When SNR approaches infinity, the theoretical limit of detection error rate is formulated by

$$P_e \overset{{\sigma_n}^2 \to 0}{=} Q\left(\frac{\sigma_a^2 D\sqrt{2M}}{\sqrt{2G^2({\sigma_n}^4 + {\sigma_a}^4 + 2{\sigma_a}^2{\sigma_n}^2) + DG{\sigma_a}^4}}\right) = Q\left(\frac{D\sqrt{2M}}{\sqrt{2G^2 + DG}}\right). \tag{21}$$

4 Algorithm Simulation and Result Analysis

This section presents the simulation and evaluation results of the SCS detection method. The impact of the number of sampling points and the frequency-domain resources occupied by the signal on performance is evaluated. The simulation results and theoretical analysis results are compared and analyzed. Simulation parameters are listed in Table 1.

Table 1. Simulation parameters.

Simulation parameter	Value
Frequency range	FR1
Modulation mode	QPSK
Bandwidth	10 MHz
Sampling frequency	15.36 MHz
Candidate SCS	15 KHz, 30 KHz
Channel modle	AWGN

4.1 Simulation Results

Simulation results and analysis are given below. The detection correct rate of different SCS with $M = 10^5$ is plotted in Fig. 1. As can be seen from Fig. 1, due to the huge number of sampling points, the proposed detection algorithm performs pretty well. When SNR is about -11 dB, the correct rate can reach 95%. When SNR is about -8 dB, the correct rate closes to 1. The detection performance of 15 kHz and 30 kHz is consistent. Furthermore, the simulation results are consistent with the theoretical analysis results.

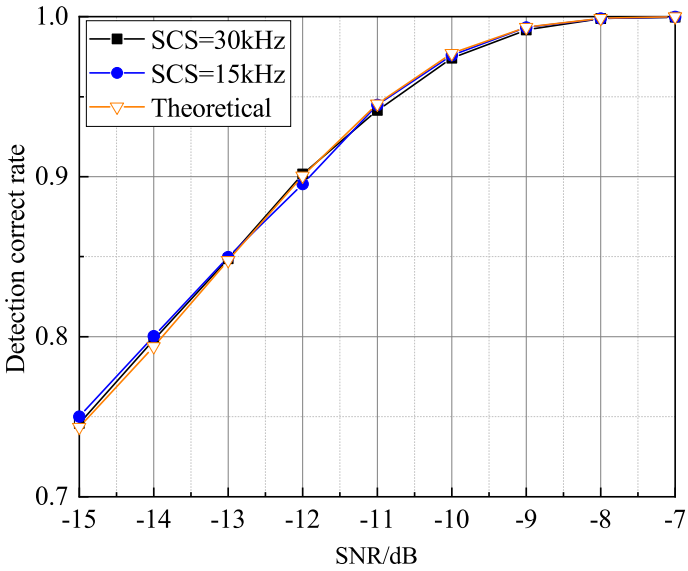

Fig. 1. The detection correct rate of different SCS with $M = 10^5$.

Figure 2 shows the detection correct rate of different SCS with $M = 1096$. As the number of sampling points used to calculate the aotocorrelation results is relatively small, the detection performance is degraded. When SNR is about 4dB,

the correct rate can reach 95%. When the SNR is in small range (SNR < 0 dB) and the detection error is primarily caused by noise, the performance of 15 kHz and 30 kHz is almost consistent with the theoretical analysis results. However, there are some errors in the limit performance between the simulation results and theoretical analysis when SNR is large. In this case, the detection performance mainly depends on the error of the useful signal autocorrelation results $R_s(N_1)$ and $R_s(N_2)$. The sampling points of time-domain sequence for correlation calculations do not obey completely independent Gaussian distributions. However, such assumptions are made in theoretical analysis. Therefore, this will cause certain error between the simulation results and theoretical analysis.

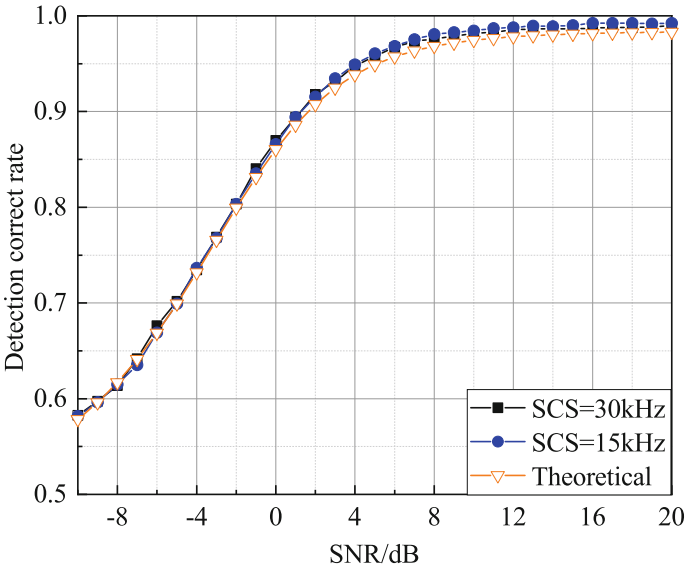

Fig. 2. The detection correct rate of different SCS with $M = 1096$.

It can be seen from Fig. 1 and Fig. 2 that the number of sampling points for autocorrelation calculation is a key factor impacting on the performance of SCS detection. Table 2 shows the detection correct rate with different M when SNR$= -10$ dB. Within a certain range, increasing M will significantly improve the detection performance and the simulation results are consistent with the conclusions of the theoretical analysis. On the other hand, the complexity of the detection algorithm $\mathcal{O}(M)$ will increase with the increase of M. Therefore, when selecting the number of sampling points for detection, both the detection performance and algorithmic complexity should be taken into account.

In the above simulation scenarios, the signal occupies all the frequency-domain resources. However, in the actual communication systems, the signal does not occupy all the sub-carriers in frequency-domain. In addition, the primary synchronization signals (PSS) in SSB block used in the synchronization

Table 2. Detection correct rate with different M when SNR = −10 dB.

Number of sampling points	Detection correct rate in simulation	Detection correct rate of theoretical analysis
1096	57.7%	57.8%
1096 × 5	67.8%	67.1%
1096 × 10	73.6%	73.4%
1096 × 50	91.7%	91.9%
1096 × 100	97.7%	97.6%
1096 × 120	98.5%	98.5%

process only occupy 127 sub-carriers in the middle of the bandwidth. The evaluations of the proposed SCS detection algorithm are given when the frequency-domain resources are not fully used.

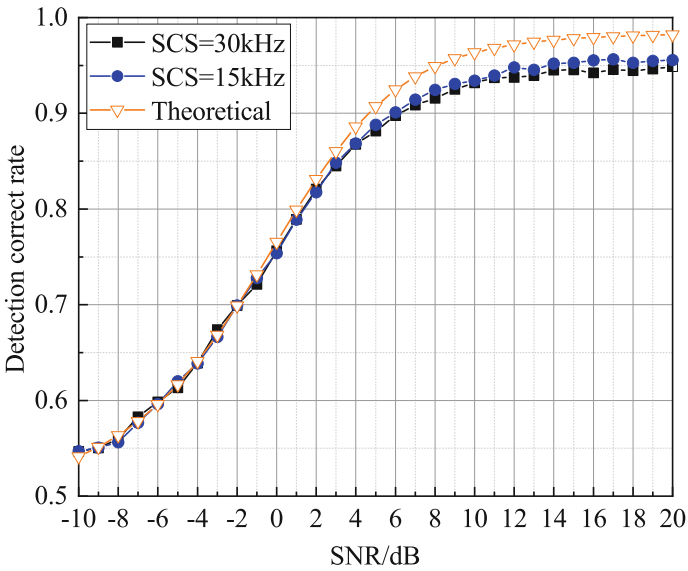

Fig. 3. The detection correct rate when the signals only occupy half of the frequency-domain resources.

Figure 3 and Fig. 4 plot the SCS detection correct rate when the signals only occupy half and one-quarter of the frequency-domain resources, respectively. The power of signal decreases as the frequency-domain resources reduces. Therefore, the theoretical analysis results are respectively 3 dB and 6 dB lower than the condition where all the frequency-domain resources are occupied. When SNR is high, the simulation performance deviates from the theoretical analysis.

When signal only occupies half of the frequency-domain resources, the theoretical highest detection correct rate is about 98.3%. And the simulation results of SCS with 15 kHz and 30 kHz are 95.5% and 94.8%, respectively. When the signal only occupies a quarter of the frequency-domain resources, the theoretical highest detection correct rate is still about 98.3%. However, the simulation results with SCS of 15 kHz and 30 kHz are 89.0% and 88.2%, respectively. As the frequency-domain resources decrease, the best performance of the proposed SCS detection algorithm gradually deteriorates. The sampling points of the signal sequence in time-domain are no longer independent when the number of subcarriers drops significantly. Moreover, the distribution of the received signal does not obey Gaussian distribution as assumed in theoretical derivation process. As a result, the variance of the correlation results also increases relative to the theoretical analysis. It can be concluded that the reduction of frequency-domain resources undermines the performance of the SCS detection algorithm.

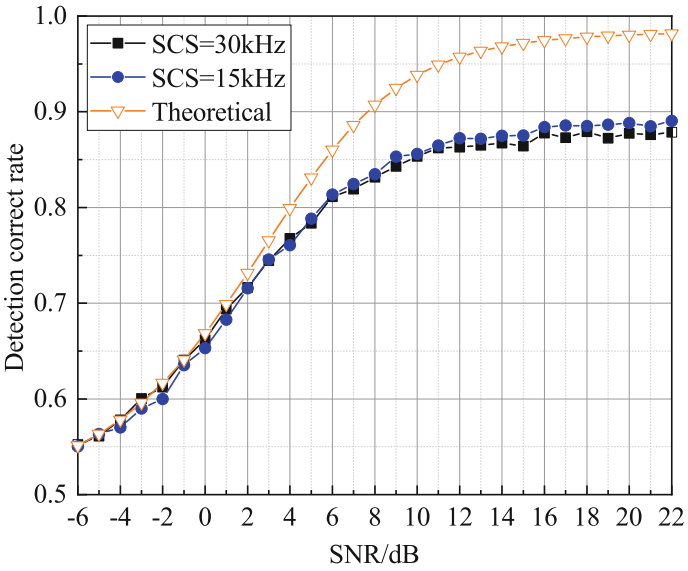

Fig. 4. The detection correct rate when the signals only occupy one-quarter of the frequency-domain resources.

Based on a large number of simulation results, the loss of performance can be analyzed quantitatively. When SNR is infinite, the noise can be ignored and the performance of SCS detection algorithm depends on the error of the correlation result $R_s(N_1)$ and $R_s(N_2)$ of the signal. According to the simulation statistics, if the useful signal occupies $\frac{1}{n}$ of all frequency-domain resources, $n \in Z$, the statistical variance of $R_s(N_1)$ increases to n times that of the theoretical analysis. For the case where the actual SCS is 30 kHz, the statistical variance of $R_s(N_2)$ increases to n times that of the theoretical analysis as well. While for the case

where the actual SCS is 15 kHz, the statistical variance of $R_s(N_2)$ increases to $\frac{n}{2}$ times that of the theoretical analysis. When the actual SCS is 15 kHz, the variance of the simulation statistics result of $R_s(N_2)$ is smaller than that of 30 kHz. If the correlation calculation is based on OFDM symbols of 15 kHz SCS with the time delay of N_2, nearly half of the sampling points for conjugate multiplication are in the same symbol. Therefore, they are not completely independent. However, if the correlation calculation is based on OFDM symbols of 30 kHz SCS with the time delay of N_2, the sampling points for conjugate multiplication are in two different symbols and they are completely independent. This is the reason why the detection performance of 15 kHz is slightly better than that of 30 kHz.

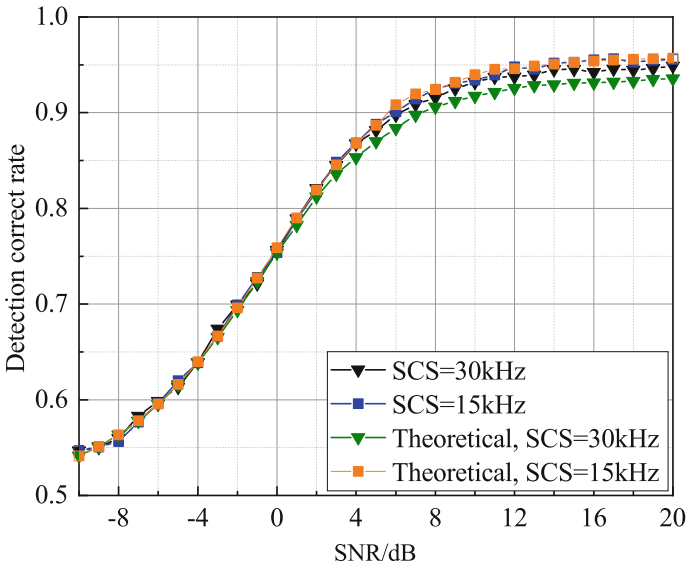

Fig. 5. The detection correct rate when the signals only occupy half of the frequency-domain resources with compensated theoretical analysis.

Based on the above simulation and analysis results, the variance of the theoretical analysis results with the SCS of 15 kHz and 30 kHz can be compensated for the situation that the signal does not occupy all the frequency-domain resources. Figure 5 and Fig. 6 show the detection performance after the compensation of the theoretical analysis results. It can be seen from the figures that the theoretical analysis result after compensation is closer to the actual simulation results, and the performance of 15 kHz is slightly better than that of 30 kHz.

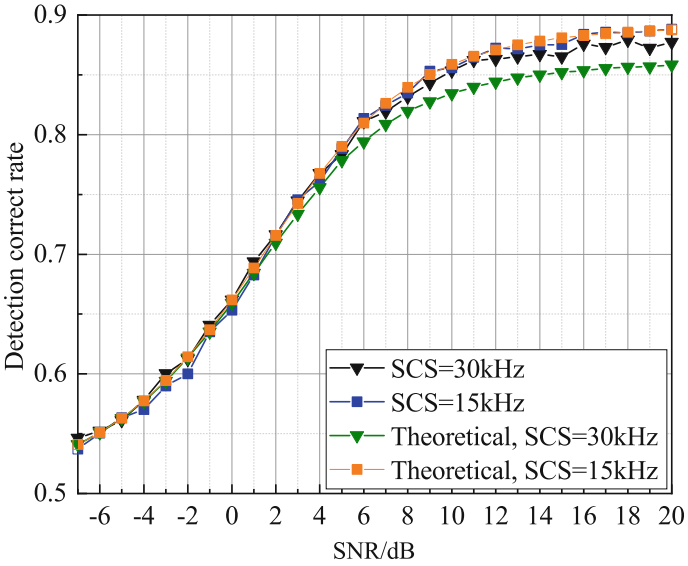

Fig. 6. The detection correct rate when the signals only occupy one-quarter of the frequency-domain resources with compensated theoretical analysis.

5 Conclusion

In 5G NR systems, UE can not get the actual SCS directly in the cell initial access process. Therefore, the SCS needs to be detected. A SCS detection algorithm based on the cyclostationarity of OFDM signals is proposed and the performance is evaluated with both simulations and theoretical analysis.

The simulation results are roughly consistent with the theoretical analysis and the detection performance of different SCS is almost symmetrical. The performance of the proposed algorithm improves as the number of sampling points and the SNR increase. According to the theoretical analysis, when the signal does not occupy all the frequency-domain resources, the performance deteriorates, which is only caused by the reduction of signal power. However, the errors excluded in theoretical analysis cannot be ignored during the actual detection process. Hence, the performance of the simulation is lower than the theoretical analysis. In this case, the theoretical analysis results can be compensated according to different SCS to make them roughly consistent with simulation results.

References

1. Liu, J., Au, K., Maaref, A.: Initial access, mobility, and user-centric multi-beam operation in 5G new radio. IEEE Commun. Mag. **56**(3), 35–41 (2018)
2. Lin, Z., Li, J., Zheng, Y.: SS/PBCH block design in 5G new radio (NR). In: 2018 IEEE Globecom Workshops (GC Wkshps), pp. 1–6 (2018)

3. 3GPP TS 38.213: 3rd Generation Partnership Project; Technical Specification Group Radio Access Network; NR; Physical layer procedures for control (Release 16)
4. Zhang, J., Li, Y.: Cyclostationarity-based symbol timing and carrier frequency offset estimation for OFDM system. In: International Conference on Computer Application and System Modeling (ICCASM 2010), Taiyuan, China, pp. V5-546–V5-550 (2010)
5. Walter, A., Eric, K., Andre, Q.: OFDM parameters estimation a time approach. In: Conference Record of the Thirty-Fourth Asilomar Conference on Signals, Systems and Computers. IEEE, Pacific Grove (2000)
6. Shi, M., Bar-Ness, Y., Su, W.: Blind OFDM systems parameters estimation for software defined radio. In: 2007 2nd IEEE International Symposium on New Frontiers in Dynamic Spectrum Access Networks. IEEE, Dublin (2007)
7. Heath, R.W., Giannakis, G.B.: Exploiting input cyclostationarity for blind channel identification in OFDM systems. IEEE Trans. Signal Process. **47**, 848–856 (1999)
8. Al-Habashna, A., Dobre, O. A.: Cyclostationarity-based detection of LTE OFDM signals for cognitive radio systems. In: 2010 IEEE Global Telecommunications Conference GLOBECOM. Miami, FL, USA (2010)
9. 3GPP TS 38.300: 3rd Generation Partnership Project; Technical Specification Group Radio Access Network; NR; NR and NG-RAN Overall Description (Release 16)
10. Li, Z.: The research about spectral correlation of subcarrier of OFDM and blind recoginition about modulation type. In: 2011 International Conference on Consumer Electronics, Communications and Networks. IEEE, Xianning (2011)